

The effect of decomposition on crystallization in $Zr_{41}Ti_{14}Cu_{12.5}Ni_{10}Be_{22.5}$ bulk metallic glass

WEI-HUA WANG*

Center for Condensed Matter Physics, Institute of Physics, Chinese Academy of Sciences, 100080 Beijing, People's Republic of China; Hahn-Meitner-Institut, Glienicke Strasse 100, D-14109 Berlin, Germany
E-mail: whw@aphy.iphy.ac.cn

Q. WEI, S. FRIEDRICH

University Potsdam, Institute Berufspädagogik, Golm, 14467 Potsdam, Germany

The decomposition as well as its effects on the crystallization of the bulk metallic glass (MG) $Zr_{41}Ti_{14}Cu_{12.5}Ni_{10}Be_{22.5}$ has been investigated using transmission electron microscopy (TEM). It is found that the decomposition destabilizes the MG and makes the MG thermally less stable with respect to crystallization. The effects of the phase separation on the subsequent crystallization are discussed based on the microstructural characteristics of the MG. © 2000 Kluwer Academic Publishers

1. Introduction

Phase separation has been found and intensively studied in metallic glasses in the last decade, it is an important factor in understanding the crystallization process and the glass forming ability (GFA) of the metallic glass (MG) [1–4]. Recently, Johnson *et al.* [5, 6] have developed a multicomponent glass forming system $Zr_{41}Ti_{14}Cu_{12.5}Ni_{10}Be_{22.5}$. The metallic glass can be obtained in various shapes and sizes even by the conventional casting process at a low cooling rate. This brings bulk MG close to technical applicability. The phase separation is discovered in the supercooled liquid state of the $Zr_{41}Ti_{14}Cu_{12.5}Ni_{10}Be_{22.5}$ MG. Intensive attention and interest has been paid to the decomposition phenomenon in the bulk MG and much effort has been devoted to this work [7–10]. The low cooling rate for the formation of the MG allows one to observe the phase separation taking place below a miscibility gap in the supercooled liquid region (SLR). It was demonstrated that the phase separation in the supercooled liquid state plays a crucial role in modulating the thermal property and modifying the microstructure in the subsequent crystallization [9–11]. Field ion microscopy with an atom probe (FIM/AP) revealed that the as-quenched $Zr_{41}Ti_{14}Cu_{12.5}Ni_{10}Be_{22.5}$ MG decomposed into Be rich and Ti rich amorphous phases in the SLR. Be and Ti show clear anti-correlated concentration fluctuations from the observation of FIM/AP, Zr, Cu, Ni do not participate significantly in the decomposition [8, 9]. However, up to now, the effects of the decomposition on the subsequent crystallization are a controversial question, because adequate experimental data concerning the effects have not been achieved, and the different experiments lead to contradictory results. The relation between the microstructural characteristics

and the decomposition of the MG is still unclear. In this work, transmission electron microscopy (TEM) is used as the main experimental method to study the decomposition as well as the influence of decomposition on the crystallization in the $Zr_{41}Ti_{14}Cu_{12.5}Ni_{10}Be_{22.5}$ MG. The effects of the decomposition on the crystallization of the alloy are discussed by using the microstructural characteristics of the MG.

2. Experimental procedure

Amorphous alloy ingots, with nominal composition $Zr_{41}Ti_{14}Cu_{12.5}Ni_{10}Be_{22.5}$, were prepared from a mixture of the elements of purity range from 99.9% to 99.99% by induction melting under a Ti-gettered Ar atmosphere. The ingots were remelted in a sealed silica tube under a pure Ar atmosphere and were subsequently water quenched, resulting in a cylindrical rod with diameter of 12 mm. The details of the preparation process of the sample was described in Ref. [10]. The cross-sectional thin foils cut from the middle of the rod were investigated by TEM. When the specimens were annealed, each of them was heated up to the desired temperature using a rate about 10 K/min. and cooled down at about 20 K/min. to ensure the same thermal history for all specimens. TEM experiments were performed in a Philips EM400 operating at 120 kV. The detail TEM experimental procedure can be seen in Ref [10].

3. Results

3.1. Decomposition of the metallic glass in the supercooled liquid state

The homogenous glass nature of the $Zr_{41}Ti_{14}Cu_{12.5}Ni_{10}Be_{22.5}$ MG was previously proved by X-ray diffraction (XRD) [12], differential scanning calorimeter (DSC) [10, 12], TEM [10] and small angle neutron scattering

* Author to whom all correspondence should be addressed.

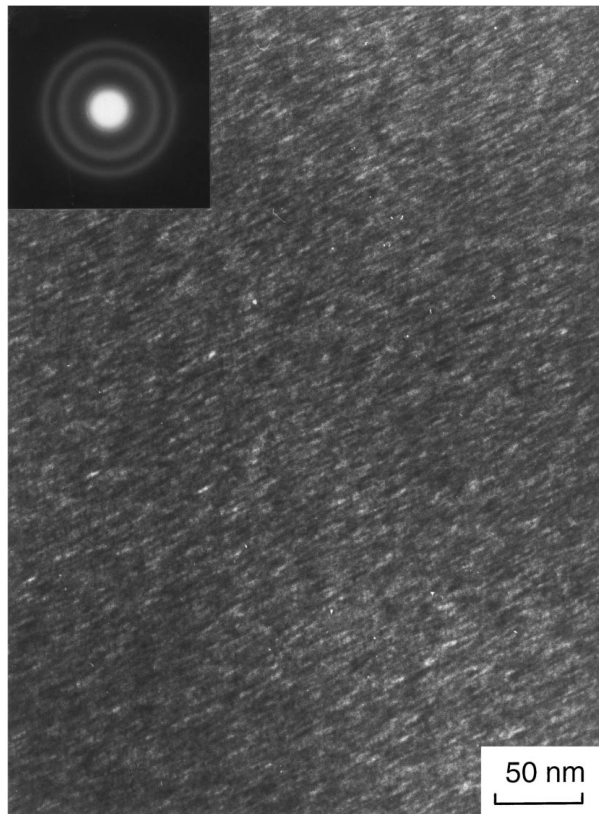


Figure 1 TEM micrograph and corresponding selected area electron diffraction pattern after annealing at 623 K for 62 h. The micrograph is taken in the light of the outer diffuse halo ring.

(SANS) [8]. The DSC results show that the MG exhibits a large supercooled liquid region, ΔT ($\Delta T = T_{x1} - T_g$ is 50 K), which is defined as the difference of the glass transition temperature T_g ($T_g = 623$ K) and the onset temperature of the first crystallization event T_{x1} ($T_{x1} = 673$ K). Fig. 1 shows a TEM dark field micrograph and the corresponding electron diffraction pattern of the MG annealed at 623 K for 62 h. The annealing temperature is just above T_g and well below T_{x1} . The alloy is in a supercooled liquid state at this annealing condition. The diffraction pattern shows two close diffuse diffraction rings resulting from the two amorphous phases in the supercooled liquid state. No sharper diffraction rings can be observed. The corresponding dark field micrograph imaged by the light of the outer ring shows that the nanosized amorphous clusters of one phase are visible in the bright contrast. The results indicate that the as-quenched MG separates into two different amorphous phases. The microstructure of the precipitates of the amorphous phase with a radius up to 3 nm embedded in the second amorphous phase matrix was also found by SANS [8]. The phase separation process in the MG was confirmed by XRD [13] and FIM/AP methods [8]. FIM/AP studies reveal that the as-quenched MG decomposed into Be rich and Ti rich amorphous phases, the Zr, Ni, Cu constituents do not participate significantly in the decomposition process.

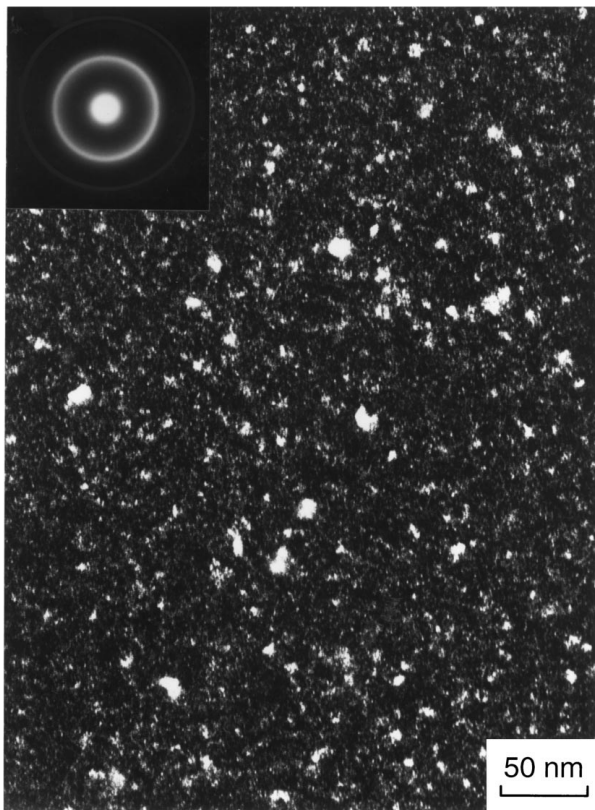
3.2. The effects of decomposition on the crystallization

In order to determine the influence of the decomposition on the crystallization behavior, the MG specimens were treated with different annealing conditions. One

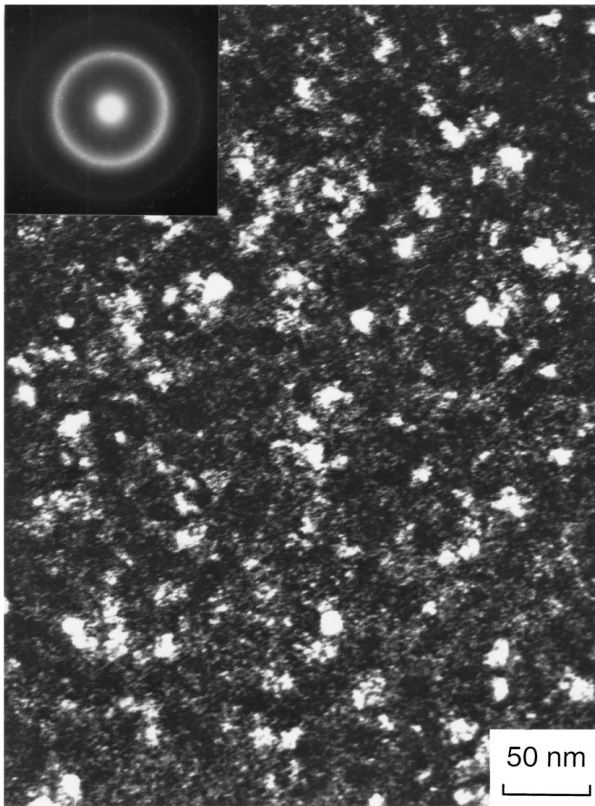
was isothermally annealed at 623 K for 15 h, and then additionally annealed at 653 K for 1 h. The isothermal anneal at 623 K for 15 h was performed to cause a decomposition of the glass prior to the crystallization, and then to exhibit the effects of the decomposition on the subsequent crystallization. (i.e. a treatment decomposition preceding crystallisation). As displayed in Fig. 2a, the Bragg peaks of the crystalline phase have been observed in the diffraction pattern after an additional anneal at 653 K for 1 h. The results indicate that the MG with decomposition preceding crystallisation partially crystallizes in the SLR. The dark field picture in Fig. 2a shows the specimen with decomposition preceding crystallisation has finer and denser nano-scale crystallites. Another specimen was directly annealed near the crystallization temperature, 673 K for 1 h. The TEM dark field picture and diffraction pattern of the specimen without a decomposition preceding crystallisation are presented in Fig. 2b. The sharp crystalline peaks arising from partial crystallization of the MG can be seen in the diffraction pattern. The dark field picture shows that various sizes of the crystallites are sparsely distributed randomly in the amorphous matrix. The size distribution of the crystallites in the specimens with and without decomposition preceding crystallisation treatment are shown in Fig. 3a and b respectively. For the specimen with the decomposition preceding crystallisation the measurement shows that the crystalline size distribution is mainly from 1 nm to 8 nm, with the average size of 2 nm. For the directly crystallized specimen, the size of the crystallites ranges from 1 to 14 nm, and the average size is 3.5 nm. The different crystallite size distributions in the two specimens result from the different nucleation processes. The crystallites in the specimen without decomposition preceding crystallisation are formed by a homogeneous nucleation due to a composition fluctuation from the initial homogeneous alloy. In contrast, the formation of the crystallites in the specimen with decomposition preceding crystallisation is influenced by the decomposition. As the phase separation proceed in the initial MG, the interfaces between the decomposed phases provide the nucleation sites and facilitate the nucleation of the crystalline phases, and the crystallites are formed by a heterogeneous nucleation process. This leads to the crystallization of the MG at a lower temperature. The decomposition preceding crystallisation thermally destabilizes the MG. TEM observation also indicates that the crystallization in the MG can undergo different paths to the crystallization. The MG can directly crystallize by nucleation and growth from the initial homogenous MG, or can decompose into two amorphous phases. The decomposed phases crystallize at a relatively lower temperature.

3.3. Thermal stability of ZrTiCuNiBe alloy with the change of Be content

To study the thermal stability of the decomposed phases and clarify the effects of the decomposition on the subsequent crystallization, the metallic glasses with different Be contents ($Zr_{41}Ti_{36.5-x}Cu_{12.5}Ni_{10}Be_x$, $15 \leq x \leq 32$ at.%), which may correspond to the decomposed



(a)



(b)

Figure 2 TEM micrograph and corresponding selected area electron diffraction patterns (a) after annealing at 623 K for 15 h, then annealing at 653 K for 1 h; (b) after annealing at 673 K for 1 h.

products, were prepared to investigate their thermal stability and GFA. Fig. 4 shows the relation of T_{x1} , T_g and the critical cooling rate of the MG with the different Be contents. It can be seen that the T_g , T_{x1} values of the

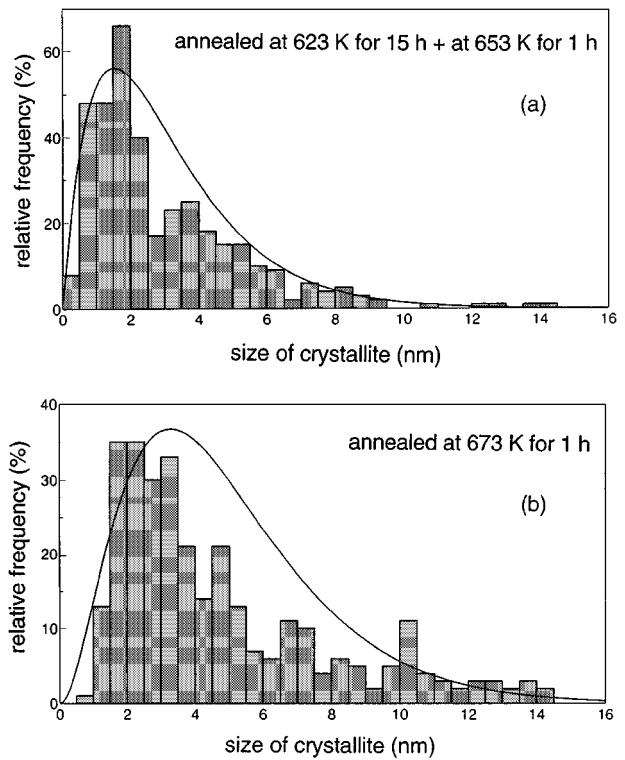


Figure 3 The size distribution of the crystallites in the MG after partial crystallization. (a) after annealing at 623 K for 15 h, then annealing at 653 K for 1 h; (b) after annealing at 673 K for 1 h.

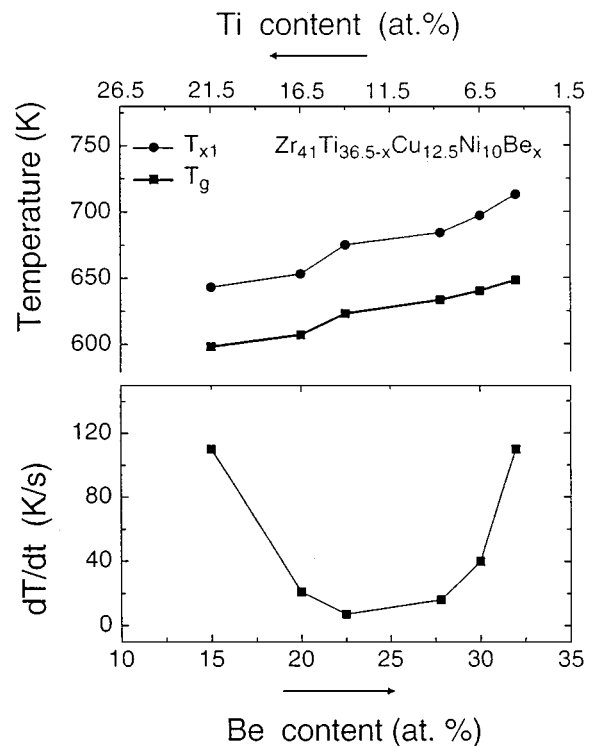


Figure 4 The changes of T_x , T_g and critical cooling rate of the $Zr_{41}Ti_{36.5-x}Cu_{12.5}Ni_{10}Be_x$ MG with different Be contents x .

MGs shift to a higher temperature with increasing Be content. The results indicate that the thermal stability of the MG is increased by adding more Be. The Be rich Zr-Ti-Cu-Ni-Be MG is thermally more stable with respect to crystallization. The critical cooling rate of the alloy system is sensitive to the Be content as shown in

the Fig. 4, the alloy with Be rich content and Ti rich content require a much higher critical cooling rates, the MG with more or less Be contents are not as good a glass former as the $Zr_{41}Ti_{14}Cu_{12.5}Ni_{10}Be_{22.5}$ MG. The MG $Zr_{41}Ti_{14}Cu_{12.5}Ni_{10}Be_{22.5}$, which can be prepared at the minimum critical cooling rate, is the best GFA defined by critical cooling rate in the ZrTiCuNiBe alloy. This confirms that Be and Ti elements play an important role in the GFA of the MG. The experimental results support the suggestion that the decomposition destabilizes the as-quenched MG and makes the MG thermally less stable with respect to crystallization, because the decomposed Ti rich phase in the MG is thermally less stable against crystallization than the as-quenched MG and crystallizes at the lower temperature relative to the as-quenched MG. The crystallization process in the decomposed MG should begin in the Ti rich amorphous phase.

3.4. The changes of the mechanical property in decomposition and crystallization

Vickers microhardness (HV) measurements were applied to confirm the effects of decomposition on the crystallization in $Zr_{41}Ti_{14}Cu_{12.5}Ni_{10}Be_{22.5}$ MG, because the HV in MG is sensitive to the structural change and phase transformation. The testing load was 1.96 Newton force. The accuracy of the measurement was about 3%. A comparison of the HV change of the MG which has undergone different heat treatments is shown in Fig. 5. The HV increases from 5.40 GPa in the as-quenched state to 6.15 GPa after the isothermal anneal at 623 K, and then shows insignificant change even for 200 h of annealing. The MG has undergone a complete decomposition during the isothermal annealing process. The result indicates that the HV of the MG is evidently affected by the phase separation before crystallization happens. When the MG is isothermally annealed at 653 K, the HV increases to a saturation value of 6.5 GPa. The increase of the HV results mainly from the full relaxation of the MG in the supercooled liquid state, the relaxation leads to the annihilation of the

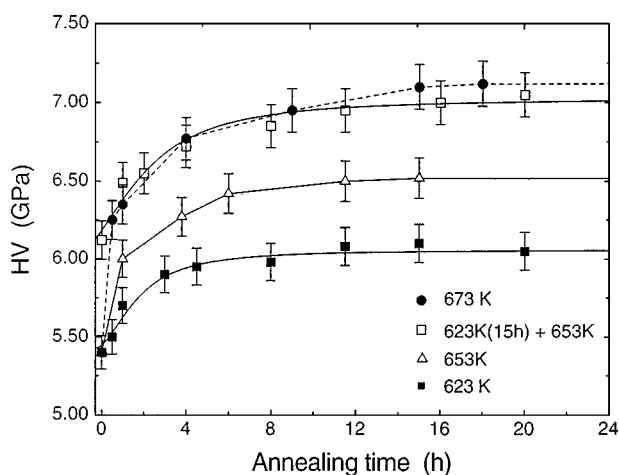


Figure 5 The HV changes of the $Zr_{41}Ti_{14}Cu_{12.5}Ni_{10}Be_{22.5}$ MG after annealing at different temperatures.

free volumes and makes a more dense randomly packed structure of the MG. To compare the HV differences in the MG with and without a decomposition preceding crystallisation, the as-quenched MG was isothermally annealed at 623 K for 15 h to cause a decomposition preceding crystallisation. When the MG with the decomposition preceding crystallisation treatment was annealed at 653 K, the HV saturation value was raised to 7.00 GPa in comparison to 6.15 GPa in supercooled liquid state and 6.50 GPa for the sample annealed at same temperature without a decomposition treatment. The HV saturation value is similar to that of the crystallized sample isothermally annealed at 673 K. The HV measurement result indicates that partial crystallization occurs in the sample with decomposition preceding crystallisation, and the crystallization gives rise to the precipitation of nanocrystallites in the MG, the nanocrystallites/amorphous mixture resulting in an enhanced HV [14, 15]. The result is taken as further evidence that the decomposition thermally destabilizes the initial MG.

4. Discussion

The TEM observation results demonstrate that phase separation occurs in the $Zr_{41}Ti_{14}Cu_{12.5}Ni_{10}Be_{22.5}$ MG. The phase separation in the supercooled liquid state means that the composition of the MG is distinct from the respective crystalline phases. The decomposed amorphous phases were found to have different short range orders compared with the as-quenched MG [16]. The results mean that the MG has significant differences in microstructure and composition compared to the corresponding crystalline compounds. Due to the complexity and large atomic size ratios in the multi-component alloy, the MG has a highly dense randomly packed microstructure, which is more closely packed than that of the conventional MG. The microstructural and compositional characteristics make the nucleation and growth of the crystalline phases from the initially homogenous supercooled liquid extremely difficult, because of the extremely slow mobility of the constituents in the highly viscous supercooled liquid. It is very difficult for the five elements in the alloy to simultaneously satisfy the compositional and structural requirements of the crystalline compounds. The origin of the excellent GFA of the MG results from the two microstructural characteristics. The experimental results confirm that a tendency to phase separation exists in the best glass former $Zr_{41}Ti_{14}Cu_{12.5}Ni_{10}Be_{22.5}$ MG, the tendency to decomposition is another contributing factor to the excellent GFA of the alloy. However, the decomposition destabilizes the MG and makes the MG thermally less stable with respect to crystallization. The conclusion is supported by the experimental data, which shows the relation of the thermal stability and the Be content of the alloy. To clarify the phenomena, a schematic plot of the free energies diagram is illustrated in Fig. 6, which exhibits schematically the decomposition and crystallization behavior of the MG. The diagram can be read as a binary cut through a multicomponent alloy with respect to Be and Ti components that the phase separation involved. The free energy curves for

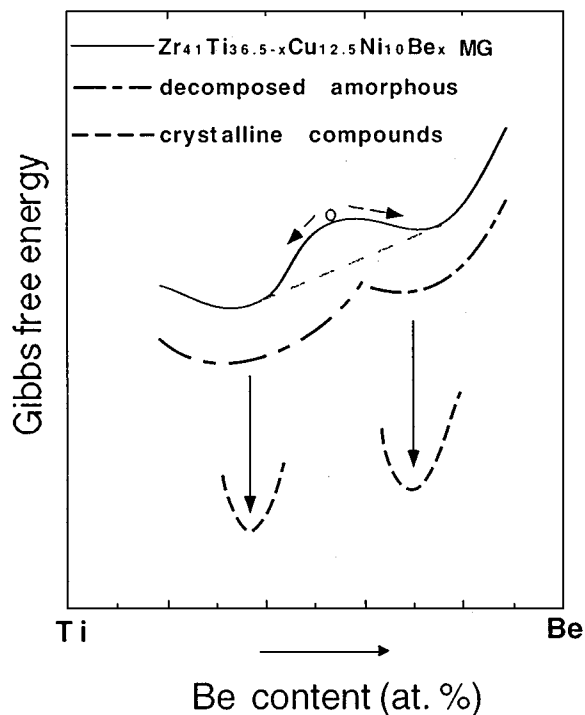


Figure 6 Schematic Gibbs free energies of a supercooled liquid, two decomposed amorphous phases and two crystalline compounds.

a supercooled liquid state of MG, two decomposed Be rich and Ti rich amorphous phases and two crystalline compounds are drawn in the figure. From the diagram, one can see that the crystallization is a non-polymorphic crystallization process, because of the microstructural and compositional differences between the MG and its corresponding crystalline phases. The MG can go towards the crystalline states along two crystallization paths. One process is the homogeneous nucleation of the crystalline compounds by a composition fluctuation directly from the initial homogenous melt. The MG can also undergo a preceding phase separation in the SLR by spinodal decomposition decomposing into two amorphous phases with no activation barrier. The decomposed phases have similar local structures and composition to the respective crystalline compounds. Thus, the subsequent crystallization process is close to polymorphic. The two processes compete in the MG towards the crystalline states. The TEM observation results demonstrate that the two crystallization phenomena do exist in the MG. Due to the larger composition and local structure difference between amorphous and crystalline compounds, the nucleation barrier is much larger for nucleation of crystalline phase directly from the homogenous MG in supercooled liquid, the nucleation needs a relatively long time scale and higher temperature. The phase separation makes the MG decompose into two amorphous phases which have similar composition and local structure to their respective crystalline compounds. The nucleation barrier decreases after the phase separation in the MG, and the subsequent crystallization is close to a polymorphic process. The nucleation probability for the formation of the compounds in the decomposed phases increases compared to that in the initial homogenous MG. The phase separation may also give rise to a great decrease

in the viscosity of the supercooled liquid and then in an increase in the mobility of the atoms in the melt [17]. Meanwhile, the interfaces induced by decomposition promote the nucleation of the crystalline phases by providing the nucleation sites. So, the crystallization path through decomposition preceding crystallisation is the kinetically favored one in the MG. The phase separation affects the subsequent crystallization by promoting the nucleation and decreasing the thermal stability of the MG.

5. Conclusion

TEM observation confirms that the decomposition occurs in the as-quenched metallic glass $Zr_{41}Ti_{14}Cu_{12.5}Ni_{10}Be_{22.5}$. The phase separation in the supercooled liquid state means that the composition of the MG is distinct from the respective crystalline phases. The decomposed amorphous phases have compositions and local structures close to the respective crystalline compounds and exhibit a high nucleation rate in crystallization compared to that of the as-quenched MG. The decomposition in the supercooled liquid region affects the subsequent crystallization by promoting the nucleation and destabilizing the thermal stability of the MG.

Acknowledgement

We would like to thank Dr. M. X. Pan for his useful discussion. One of the author (W. H. Wang) is grateful to the grant of the Alexander von Humboldt Foundation in Germany.

References

1. L. E. TANNER and R. RAY, *Scr. Metall.* **14** (1980) 657.
2. D. DENG and A. S. ARGON, *Acta Metall.* **10** (1986) 2011.
3. R. BORMANN, F. GAERTNER and F. HAIDER, *Mater. Sci. Eng.* **97** (1988) 79.
4. A. H. OKUMZRA, A. INOUE and T. MASUMOTO, *Acta Metall. Mater.* **41** (1993) 915.
5. W. L. JOHNSON, *Mater. Sci. Forum* **225–227** (1996) 35.
6. A. PEKER and W. L. JOHNSON, *Appl. Phys. Lett.* **63** (1993) 2342.
7. R. BUSCH, Y. J. KIM and W. L. JOHNSON, *J. Appl. Phys.* **77** (1995) 4039.
8. A. WIEDENMANN, U. KEIDERLING, M.-P. MACHT and H. WOLLENBERGER, *Mater. Sci. Forum.* **225–227** (1996) 71.
9. M.-P. MACHT, N. WANDERKA, A. WIEDENMANN, H. WOLLENBERGER, Q. WEI, H. J. FECHT and S. G. KLOSE, *Mat. Res. Soc. Symp. Proc.* **398** (1996) 375.
10. Q. WEI, Ph.D. thesis, Potsdam University, 1997.
11. R. BUSCH, S. SCHNEIDER, A. PEKER and W. L. JOHNSON, *Appl. Phys. Lett.* **67** (1995) 1544.
12. W. H. WANG, Q. WEI and H. Y. BAI, *Appl. Phys. Lett.* **71** (1997) 58.
13. S. G. KLOSE, Ph.D. thesis, Berlin Technical University, 1995.
14. J. S. KOEHIER, *Phys. Rev. B* **2** (1970) 547.
15. P. S. FRANKWICZ, S. RAM and H. J. FECHT, *Appl. Phys. Lett.* **68** (1996) 2825.
16. W. H. WANG, Q. WEI, S. FRIEDRICH, M. P. MACHT and H. WOLLENBERGER, *ibid.* **71** (1997) 1053.
17. W. VOGEL, *J. Non-cryst. Solids* **24** (1977) 172.
18. F. SPAEPEN, R. B. MEYER, *Sci. Metall.* **10** (1976) 257.

Received 20 October 1998

and accepted 1 November 1999